DOI:10.3969/j.issn.1005-202X.2017.12.007

医学影像物理

小鼠颅骨视窗及其在光学活体脑成像研究中的应用

万小芳[1],吴金波[2],翟鹏[3],应明[2],周洁[1],王晓梅[3],屈军乐[1],许改霞[1]
1.深圳大学光电工程学院,广东省/教育部光电子器件与系统重点实验室,深圳市生物医学光学微纳检测与成像重点实验室,广东 深圳 518060;2.深圳大学生命科学学院,广东 深圳 518060;3.深圳大学医学院,深圳市生物医学工程重点实验室,广东 深圳 518060

【摘 要】小鼠颅骨视窗作为一种活体光学脑成像辅助工具,以其原位表征、实时观察、长期活体脑成像等优势,成为脑部疾病及神经元突触生长等研究的重要手段之一。小鼠颅骨视窗不仅可以对颅骨下软脑膜血管及血管内红细胞流速、流态变化进行定量分析,在结合荧光标记物与光学显微镜后,还可以对脑部皮层下组织、神经细胞的变化进行清晰成像。过去数十年,科研人员利用小鼠颅骨视窗深入研究了偏头痛、阿尔兹海默症、神经突触等病理生理过程,并取得了大量突破性进展。同时,随着光学成像工具性能的提升,小鼠颅骨视窗的应用也得到了进一步拓展。本文主要介绍颅骨视窗的发展史、构建方法,结合荧光探针及光学成像方法的研究,全面总结了近年来小鼠颅骨视窗在光学脑成像研究中的应用,包括脑内重要生物分子成像、细胞成像、血管及血流成像、神经环路可塑性及神经功能成像、疾病发生机理及药物开发研究等,最后讨论了小鼠颅骨视窗在实际应用中面临的问题,并对其未来应用进行了展望。

【关键词】颅骨视窗;活体脑成像;阿尔兹海默症;神经环路
【中图分类号】R319 【文献标志码】A 【文章编号】1005-202X(2017)12-1220-12

Cranial window in mouse and its application for optical brain imaging *in vivo*

WAN Xiaofang[1], WU Jinbo[2], ZHAI Peng[3], YING Ming[2], ZHOU Jie[1], WANG Xiaomei[3], QU Junle[1], XU Gaixia[1]
1. Key Laboratory of Biomedical Optical Micro-Nano Measuring and Imaging of Shenzhen, Key Laboratory of Optoelectronic Devices and System of the Ministry of Education/Guangdong Province, College of Optoelectronic Engineering, Shenzhen University, Shenzhen 518060, China; 2. College of Life Science, Shenzhen University, Shenzhen 518060, China; 3. Key Laboratory of Biomedical Engineering of Shenzhen, School of Medicine, Shenzhen University, Shenzhen 518060, China

Abstract: Cranial window in mouse, as a kind of *in vivo* optical imaging aided instrument, with the advantages of *in situ* representation, real time observation and long-term imaging, has became one of the most important methods for the research of brain diseases and synapse growth. The cranial window can be used to visualize the leptomeningeal vessels and quantitatively analyze the flow velocity and flow regime changes of the erythrocytes in blood vessels. Moreover, combined with the fluorescent markers and optical microscopes, the cranial window can be applied for obtaining the clear images of the brain cortical tissue and the neurons. Over the past few decades, with the aid of cranial window, researchers made lots of breakthroughs on the studies of migraine, Alzheimer's disease and the synapses. Recently, with the development of optical imaging tools, the application of cranial window had been further expanded. Herein, the history of cranial window and construction methods were introduced. We also reviewed the applications of cranial window combined with the fluorescent markers and optical microscopes on optical brain imaging (including imaging for important biological molecules in brain, cells, blood vessels, blood flow, plasticity of neural circuits and neurological functions, and research for pathogenesis and drug screening). Finally, the challenges of different cranial windows in practical application were discussed and the future applications of optical cranial window were prospected.

Keywords: cranial window; *in vivo* brain imaging; Alzheimer's disease; neural circuits

【收稿日期】2017-07-17
【基金项目】国家重点基础研究发展计划(973计划)(2015CB352005);国家自然科学基金(31671491,61405169);广东省自然科学基金(2014A030312008);国家级大学生创新训练资助项目(201410590036);中国博士后科学基金(2016M602523)
【作者简介】万小芳,硕士研究生,研究方向:生物光子学,E-mail: wanxiaofang2016@email.szu.edu.cn
【通信作者】许改霞,博士,教授,研究方向:生物光子学,E-mail: xugaixia@szu.edu.cn

前 言

大脑是动物体内最精细、最复杂的器官，脑功能与脑内微细结构成像也一直是科研人员研究的热点，但由于颅骨的阻隔，脑部的活体成像研究难以开展，而在活体水平对大脑活动进行实时跟踪研究更加困难。小鼠脑部颅骨视窗技术始于20世纪30年代左右，60年代逐步发展成熟，是活体脑成像的有效辅助手段[1]。颅骨视窗技术是指将颅骨移除或削薄，进而对大脑组织进行观察的一种方法。构建成功的颅骨视窗可清晰地观察到大脑表面细胞和毛细血管等，若结合双光子荧光显微镜，还可对深层脑组织进行成像，更重要的是可以进行长时间动态观察，实时了解神经细胞和组织形态结构变化，进而研究这些变化与疾病或行为变化之间的相关性[2-3]。颅骨视窗在药物研究中能更直接地观察到药物的药效发挥过程和药物对神经细胞的影响，缩短药物研发过程[4]；在对脑部疾病（如阿尔兹海默症、脑中风等）研究中，可直接观察活体小动物模型脑内小胶质细胞迁移、淀粉样蛋白斑块生长、血流速度/血细胞数量变化等，甚至利用光学技术对脑内局部进行操控，从而更深刻地了解大脑在分子层面的工作机理；在对大脑神经元结构和功能的研究中，可以借助该技术实现神经元的高分辨动态成像[5-6]。本文从颅骨视窗的发展历史、构建方法、荧光标记物、光学成像技术及其在脑成像研究中的应用等几方面展开论述，并探讨了这种实时、原位、长时间成像的技术手段在脑科学研究的应用前景。

1 颅骨视窗的发展

颅骨视窗技术使科技人员能够使用较便宜的啮齿目动物，对颅内局部微循环和脑功能信息变化进行实时观察，而随着成像方法和标记材料的不断改进，颅骨视窗的图像质量、空间分辨率、时间分辨率和成像深度都有了大幅度的提升，相关技术对于脑部功能、疾病或药物开发都有重要意义。颅骨视窗技术最早被描述于1928年Forbes研究中[7]，早期的制备技术粗糙，实验动物易感染，成像效果差，成功率较低。随后的20多年，开放式颅骨视窗技术被不断完善，研究人员将颅骨剖开后去除脑膜，将玻璃直接嵌在颅骨缺口进行观察，虽然实验过程仍会受到局部脑压过大导致脑部膨胀等问题的困扰，但成功率较之前已有明显提升[1]。实验动物也从刚开始的较大型的狗、猫、兔子转变为小型的大鼠、小鼠等。为预防由于CO_2流失所导致的脑疝，科研人员引入了流体灌注技术，降低视窗构建对脑组织造成的影响。1980年，Kuschinsky和Wahl构建了封闭式颅骨视窗，通过灌注人工脑脊液维持局部生理环境稳定性，从而使颅骨视窗模型更加接近自然状态下的脑内环境，有利于长时间活体脑成像[8]。

早期的开放式颅骨视窗技术只允许较短时间观察，时间稍长就会因为脑压改变而导致脑组织膨胀、结构破坏、功能失常，从而使窗口环境受到破坏而失去观察价值。而后发展起来的封闭式颅骨视窗技术则避免了脑组织直接暴露于环境，对实验鼠的危害减小，可以多次、长期重复观察，因此封闭式视窗迅速取代开颅式视窗成为研究颅内循环以及血管渗透性的首选。然而，在对脑内神经元突触的精细结构进行观察时，发现即使使用封闭式颅窗，在进行开颅手术时仍会不可避免地诱发脑内炎症响应，激活小胶质细胞和星形胶质细胞，导致树突棘的翻转或萎缩，引起神经元生理机能变化[2]。为了减少去除颅骨对脑内神经组织带来的影响，2002年，Grutzendler等[2]在封闭式颅骨视窗的基础上开发出薄颅技术，即不将颅骨钻开而是逐层削薄至内部血管、突触等清晰可见的程度，进一步减小对脑部的伤害和影响，但是这种方法所制备的视窗成像面积较小，且由于颅骨生长会造成表面不平整、厚度增加，成像质量变差，在实验过程中需多次打磨窗口。Drew等[9]在薄颅技术的基础上做了进一步的改进，他们首先将颅骨磨薄至更薄，而后将玻璃片粘合于打磨区域，由于玻璃会抑制颅骨生长，故在长时间观察时可以不进行反复磨薄，该方法既避免了炎症反应，又保证了长时间测量过程中优质的成像质量，是目前性能最优的一种颅骨视窗。

2 颅骨视窗的构建

成功构建颅骨视窗是其生物医学应用的基本保障。目前常用的颅骨视窗有3种类型，分别是开颅式视窗、封闭式视窗以及薄颅式视窗。这3种视窗构建的前期准备工作大致类似[2]：实验鼠以3~6周龄为佳，手术过程保持用气体麻醉（在氧气中加入3%异氟醚）[10]，使用眼药水使实验动物眼睛时刻保持湿润以防止脱水造成永久性伤害，鼠体下方加热垫为实验鼠保持体温，实验中连续监测呼吸频度及直肠温度等基本体征。手术前配制好人工脑脊液备用，用动物脑定位仪固定头部，用小型电剃刀或剪刀小心除去头皮上毛发，涂抹聚维酮碘进行消毒后，小心剪开颅骨上方头皮，接下来，即可根据需要制备颅骨视窗[9, 11]。下面简单介绍这3种视窗的构建方法。

Levasseur等[12]发展了开颅式视窗，直接用圆环状带锯齿钻头钻出观察区域，或用更小而尖锐的钻

头钻出实验区域，后一种方法目前更常见。钻头尺寸一般不超过0.5 mm，越小越易于操控并可减小对实验动物的伤害，在手术过程中需用人工脑脊液随时洗去产生的粉末。

封闭式视窗与开放式视窗主要的区别在于暴露的脑部组织有无玻片保护。具体来讲，在制备封闭式视窗时，首先需在将要研究的视窗区域周围涂抹上牙科丙烯酸酯并嵌入微型聚乙烯管（以灌注人工脑脊液），待其凝结后使用电钻小心除去颅骨（骨出血可使用骨蜡止血），在牙科丙烯酸酯围成的区域上放置玻片，使玻片粘附并与牙科丙烯酸酯密封，通过聚乙烯管灌注人工脑脊液维持脑压[13]。

与封闭式视窗相同，薄颅式视窗也能保证颅内环境的稳定性，且不需要去除颅骨，而是使用小钻头在一小区域削薄颅骨，再用玻片放置于削薄区域密封[3, 11, 14-15]。然而其成像视野小、需反复打磨等固有缺陷影响了薄颅式视窗的进一步应用。Drew等[9]发展了打磨强化薄颅视窗（Polished and Reinforced Thinned Skull, PoRTS），将成像视野拓展至2~3 mm，医用氰基丙烯酸盐水泥和玻璃形成的视窗抑制了颅骨的生长，构建的视窗几乎不会引起小鼠脑内的炎性响应，3个月后仍可对脑内荧光标记的血管进行清晰成像（图1）。

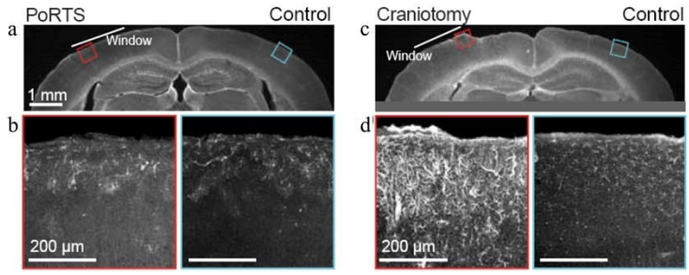

PoRTS: Polished and reinforced thinned skull; GFAP: Glial fibrillary acidic protein; Fig.1a was a wide-field image of brain slice stained for GFAP at 2 weeks after PoRTS window implantation. White line showed the extent of PoRTS window on the left. Red and blue squares denoted the regions enlarged in panel B. Fig.1b was the confocal image of GFAP staining underneath PoRTS window (left) and control contralateral hemisphere (right), showing similar basal levels of GFAP expression. Fig.1c was a wide-field image of brain slice stained for GFAP at 2 weeks after closed cranial window. White line showed the extent of cranial window on the left. Red and blue squares denote the regions enlarged in panel D. Fig.1d was the confocal image of GFAP under cranial window (left) and control contralateral hemisphere (right), showing increased levels of GFAP staining under cranial window.

图1 在PoRTS和封闭式颅骨视窗下观察脑内胶质原纤维酸性蛋白表达

Fig.1 GFAP expression under a PoRTS window and a closed cranial window

封闭式以及薄颅式视窗制作完成后，小鼠可放回鼠笼，定时监测直至其苏醒。若观察有任何疼痛的症状（如不愿动、不吃不喝、竖毛、流涎、呼吸异常等），需继续施以麻醉剂，通常长时间动态监测应在术后待实验动物情况稳定下来再进行，观察时间可长达数月甚至数年[16]。

开放式颅骨视窗是最早建立的颅骨视窗，该方法将颅骨剖开暴露出脑组织直接观察，鉴于对大脑的严重伤害，只能在建立完成后数小时内进行单次的观察分析，提供的信息有限。随着成像系统的发展、设备精度的提高，该方法现已基本废弃不用。目前，研究人员主要根据观察对象、观察周期的要求，选用封闭式和薄颅式两种颅视窗（表1）。

3 视窗荧光探针发展

早期颅骨视窗主要在白光宽场显微镜下，观察脑皮层表面局部组织形态的变化。随着荧光显微成像技术的发展，颅骨视窗的应用领域也越来越广泛。1993年，Rovainen等[17]将异硫氰酸荧光素（Fluorescein Isothiocyanate, FITC）引入到颅骨视窗用于观察脑皮层血管情况，提高成像对比度。之后，随着绿色荧光蛋白[18]及其多种突变体的发明[19-20]，荧光蛋白标记成为脑视窗成像研究中的重要手段，这种基因编码的荧光探针，可以完全消除外源性标记物对活细胞和活体动物的影响，能够稳定遗传，并可以与其它蛋白整合而不丢失荧光特性，从而对细胞内特异性结构和分子进行标记。多种突变体在受激后可以发出不同波段的荧光，实现多色标记。神经科学是荧光蛋白发明的最大受益领域之一[21]，活体小动物可以在清醒的自然情况下完成光学成像，进一步扩展了荧光成像应用的广度与深度[2, 9]。此外，近年来发展迅速的纳米技术也被应用于颅骨视窗成像，并发挥了一定的作用，本文重点介绍基因编码的荧光蛋白在颅骨视窗中的应用。

表1 两种常用颅骨视窗的比较

Tab.1 Comparison of two kinds of cranial windows

Type	Operation	Field of view/mm	Available time	Disadvantages
Closed	Drill to remove the parietal	1.0-10.0	Several months (Except the beginning and the end)	Inflammation (Anti-inflammatory antibacterials need to be used.)
Thinned	Thinner skull by drill polishing	0.2-2.0	From several months to 2 years (Image quality was not good in the later period.)	Skull regeneration affected image quality, and sometimes the skull need to be polished repeatedly.

3.1 荧光蛋白用于观察神经元形态

2002年,Grutzendler等[2]利用荧光蛋白转基因小鼠研究了脑皮层神经元细胞的发育和可塑性。小鼠的脑皮层锥体细胞表达黄色荧光蛋白,通过构建薄颅视窗,结合双光子荧光显微成像系统,研究人员观察到在数小时内,幼年小鼠的脑皮层中树突会出现伪足状突起、延伸和收缩(图2),但是在成年鼠中未发现类似现象。在视觉形成的关键期,73%的幼年小鼠在一个月的时间段里树突脊基本无变化;而对于成年小鼠,96%的树突脊在一个月内稳定无变化,树突脊消失的半衰期为2个月,这一结果表明,在发育期具有可塑性的脊柱,在进入成年后会变得稳定,该成果对于研究脑神经的记忆功能具有重要的意义。

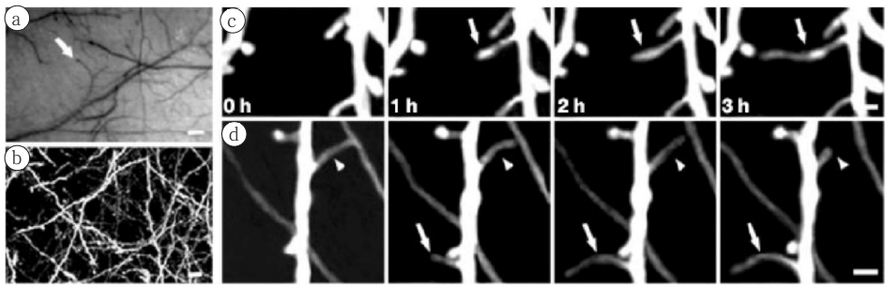

Fig.2a was the vasculature below the thinned skull observed with charge-coupled device camera view, and the arrow indicated the region where subsequent two-photon images were obtained. Fig.2b was a two-dimensional projection of a three-dimensional stack of dendritic branches and axons in the primary visual cortex. Fig.2c and d showed the time-lapse images (one-hour intervals) in two 1-month-old mice, which revealed that filopodia underwent rapid extension (arrows) and retraction (arrowheads), whereas spines on the same dendritic.

图2 幼龄小鼠神经树突伪足生长观察

Fig.2 Dynamic dendritic filopodia in the transcranial two-photon images of young mice

3.2 荧光蛋白用于脑肿瘤转移动态过程研究

肿瘤脑转移的致死率非常高,因此研究单个肿瘤细胞在脑内血管中的运动、捕获、浸润等过程,对于揭示肿瘤脑内转移发生机理具有重要意义。2010年,Kienast等[22]用红色荧光蛋白转染了PC14-PE6肺癌细胞和MDA-MB-435黑色素瘤细胞,并利用颅骨视窗研究了两种细胞在脑内转移的过程(图3)。研究人员利用双光子显微成像技术研究了两种肿瘤细胞在小鼠脑部的扩散、转移和增殖过程,发现了产生肿瘤和转移灶的几个重要步骤:肿瘤细胞在血管分支处被捕获;主动渗出扩散到旁边血管分支;在血管周围固定,进入休眠期;沿着血管与血管共生(图3d)。在最后一步中肺癌细胞与黑色素瘤细胞增殖生长的方式不同,PC14-PE6肺癌细胞会分散成几个小的细胞簇,并同步增殖后融合成一团(图3a),而MDA-MB-435黑色素瘤细胞则是从单个微型细胞簇(大约4~50个细胞)开始增殖(图3b)。观察中发现单个细胞簇增殖的方式有可能会因为缺乏新的血管形成而消退(图3c),而采用多个细胞簇同步增殖策略的往往较容易产生新的转移灶,通过抑制血管内皮生长因子-A来抑制诱导肺的长期休眠转血可有效阻止癌细胞的转移扩散。

3.3 荧光蛋白用于检测神经元动作电位

神经元细胞是一种可兴奋性细胞,当细胞兴奋时动作电位会发生改变,从而进一步引起细胞内钙离子浓度快速变化,通过钙离子成像可以跟踪神经

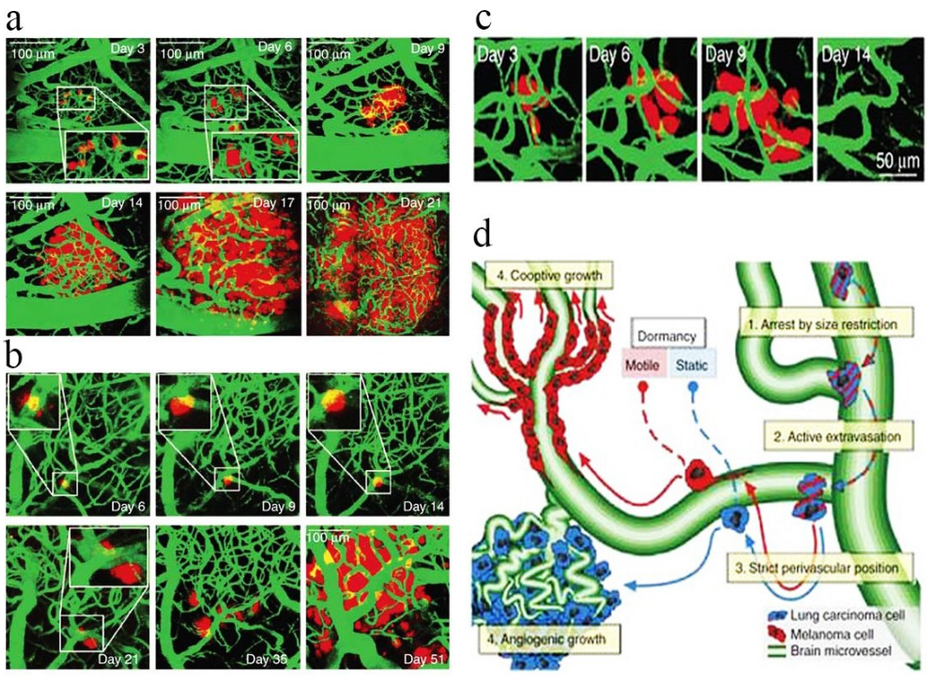

In Fig.3a, five foci of extravasated PC14-PE6 lung carcinoma cells in close proximity to each other on day 3 merged into one growing macrometastasis on day 9 (depth: 50-450 μm). In Fig.3b, macrometastasis was formed by an MDA-MB-435 melanoma cell and there was a slower growth along preexisting blood vessels (depth: 50-350 μm). In Fig.3c, a PC14-PE6 lung carcinoma micrometastasis regressed on day 14, and there were no vascular changes (depth: 0-100 μm). Fig.3d was a schematic overview of the 4 essential steps of brain metastasis formation.

图3 成功与失败转移灶的形成以及脑内转移灶形成的4个基本步骤的示意图

Fig.3 Formation of successful and unsuccessful metastatic lesions and the 4 basic steps of the formation of brain metastasis

元的活性和兴奋状态。遗传编码的蛋白质探针可以靶向标记特定神经细胞，提供神经元之间相互作用的非侵入式成像。然而已知的单荧光探针GCaMP和基于荧光共振能量转移的蛋白质探针家族在灵敏度和速度上都低于人工合成的荧光探针，于是Chen等[23]通过诱变并筛选GCaMP变体，得到超敏感的蛋白质探针家族GCaMP6。在锥体神经元2/3层处，GCaMP6能可靠地检测到神经元胞体的单一动作电位（检测率高达99.0%±0.2%）和个别树突棘方向调整引起的钙离子浓度微弱变化[23]。在视觉皮层测得GCaMP6s的响应时间为75~100 ms，GCaMP6m的响应时间50~75 ms，都低于100~150 ms的单个电位时长，意味着GCaMP6探针能近乎百分百地探测到锥体细胞动作电位，这一研究对于人类进一步了解神经元活动意义重大。

3.4 荧光蛋白用于活体脑成像

早期颅骨视窗仅用于观察脑皮层表面的局部组织形态的变化，主要使用白光反射成像模式，随着显微镜技术的不断成熟以及新型染料的出现，研究人员在1994年将荧光成像方法引入脊背视窗研究中，随后这种手段也运用于颅骨视窗中。结合双光子激发激光扫描显微镜，研究人员对小鼠脑皮层的血管系统和神经元结构进行了高分辨率成像（图4）[14]，Kelly等[15]和Guo等[24]采用跨颅双光子激光扫描显微镜研究多巴胺耗竭引起的突触重塑过程，颅骨视窗的观察范围由表面推进到组织深层，可实现对特异性分子或组织结构的高分辨率成像，深可达300 μm[2]，基因编码荧光蛋白已被用于大脑皮层神经元群的结构成像，使研究人员可以实时观测活神经元及神经突触蛋白的动力学特点[9]。荧光成像方法在颅骨视窗的应用极大地推动了脑科学的深入研究[6, 16]。

3.5 光敏感通道蛋白用于脑活动调控与成像

光遗传学技术是基因技术、光控技术及荧光成像技术结合之后的新技术。人们可以借助光遗传学技术对活体组织的特定细胞进行调控，开启或关闭某个细胞功能。光遗传在活体脑成像与神经控制方面起着重要作用。Cheng等[25]利用光遗传方法研究中风问题，在Thy-1-ChR2-YFP line-18转基因小鼠（初级运动皮层V层锥体神经元处高表达光敏感通道蛋白）的初级运动皮层受损侧（Ipsilesional Primary

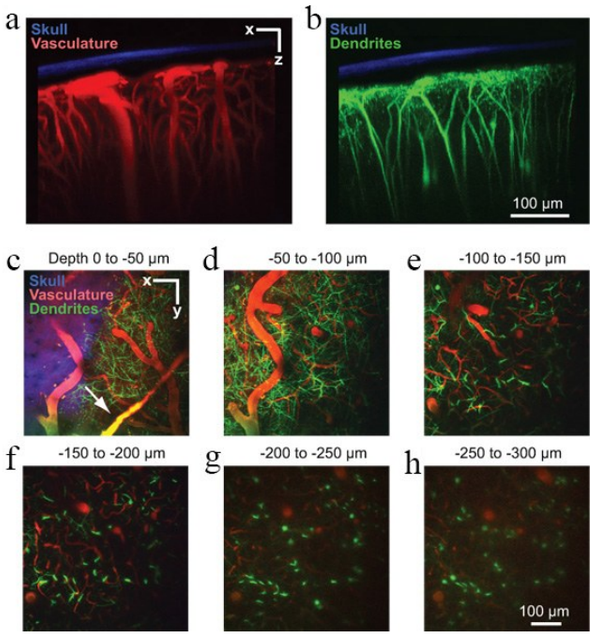

All images were collected through a PoRTS window in a Thy1-YFP mouse at 2 days after window implantation. Maximal projection over 150 μm of tissue in the coronal orientation showed the thinned skull in relation to the vasculature (Fig.4a) and dendrites (Fig.4b). The bone (blue) was detected by collecting the second harmonic fluorescence at 450 nm emission with 900 nm excitation. The vasculature (red) was labeled by intravenously injecting 70 kDa Texas-Red dextran. The dendritic fields of neurons (green) were endogenous to the Thy1-YFP transgenic mouse line. Fig.4c-h were the maximal projections over 50 μm of tissue in the horizontal orientation at different depths below the pia. Data were from the same image stack shown in panels A and B. Dural vessels may be visible just above the cortical surface (arrow in Fig.4c).

图4 双光子成像系统对小鼠大脑脑皮质血管及神经元成像

Fig.4 Vascular and neuronal imaging with two-photon imaging system in cerebral cortex of mice

Motor Cortex, iM1)给予3个连续的1 min激光刺激(3 min休息间隔),发现刺激该区域可激活周围梗死区以及对侧相同区域。结果表明,实验初期,收到重复神经刺激中风小鼠的脑血流和神经血管耦合响应显著改进,但是在中风的第五天没有明显变化,而中风的第十五天又表现出改善的迹象。重复的神经刺激可以引起运动神经元的强烈活动,肉眼下即可看到患肢的运动;重复的神经刺激还导致对侧皮层活性依赖性神经营养因子,包括脑源性神经营养因子,神经生长因子和神经营养因子-3的表达增加。蛋白分析还表明,受刺激小鼠表达可塑性标记物生长相关蛋白-43。此外,刺激正常的非中风小鼠没有改变运动行为或神经营养因子表达。虽观测到脑内梗死区域未发生变化,但iM1区域的重复神经刺激能促使中风的老鼠的体质量恢复,且在中风的第七天和第十天,与对照组(无神经刺激的中风老鼠)相比,实验组小鼠可行进更长距离,行进速度更快,表明其运动功能有明显改善。有趣的是,刺激并不改变正常无中风小鼠的运动行为或神经营养因子表达。这项研究为临床中风治疗提供了全新的思路,是脑部疾病治疗研究中开创性的成果。

4 颅骨视窗的光学成像方法

早期的颅骨视窗利用反射式光学显微镜或普通荧光显微镜对脑部进行成像,仅能提供脑组织表面信息,如微血管通透性、血管直径、神经元细胞变形等信息[12-13]。随着人类对大脑认识的深入,生物学家希望能够在活体层面研究深层脑组织、感兴趣细胞、特殊结构等的时间与空间相关性[26],因此,多种光学成像方法与颅骨视窗的结合成为近年来活体脑成像研究的热点。

4.1 多光子显微镜成像

多光子显微成像具有其独特的优点(成像光热效应和光毒性效应大幅大降,采用近红外激发可以将成像深度扩展至毫米量级),现已被用于研究肿瘤等疾病的病理状况进展和潜在治疗阿尔茨海默病,以及对评估药物治疗效果的评估[2, 27-28]。Horton等[5]设计了一种非侵入性、高分辨率的三光子荧光显微镜,利用1 700 nm的激光对小鼠大脑进行成像,可获得脑内皮质下神经元、血管等的微观结构信息(图5)。髓鞘的轴突外囊(也称为"白质")产生明亮的3次谐波生成信号,描绘了外部的边界。图像显示外囊开始于大脑表面以下840 μm,厚度大于116 μm,海马的CA1区域始于大脑皮层956 μm以下。这种多光子显微镜能够对散射组织进行高分辨率、高对比度成像,同时可以将成像拓展到皮下更新的层面,有助于活体脑内活动的实时成像。

4.2 光学相干断层扫描(Opticalcoherencetomography, OCT)成像

OCT被用于组织的高分辨率三维成像。OCT具备毫米级的成像视野和微米级的空间分辨率,已被广泛应用于脑成像。2013年,Srinivasan等[29]开发了一种多参量OCT方法,借助薄颅强化型脑视窗,研究缺血性中的小鼠皮质组织的急性损伤与慢性恢复进程。研究人员构建了细丝中脑动脉闭塞模型(filament Middle Cerebral Artery Occlusion, fMCAO),测量闭塞前、闭塞中和再灌注60 min之后(左、中、右)血管、细胞散射以及OCT信号与深度信息的比率(图6)。该方法提供了类似于多参量核磁

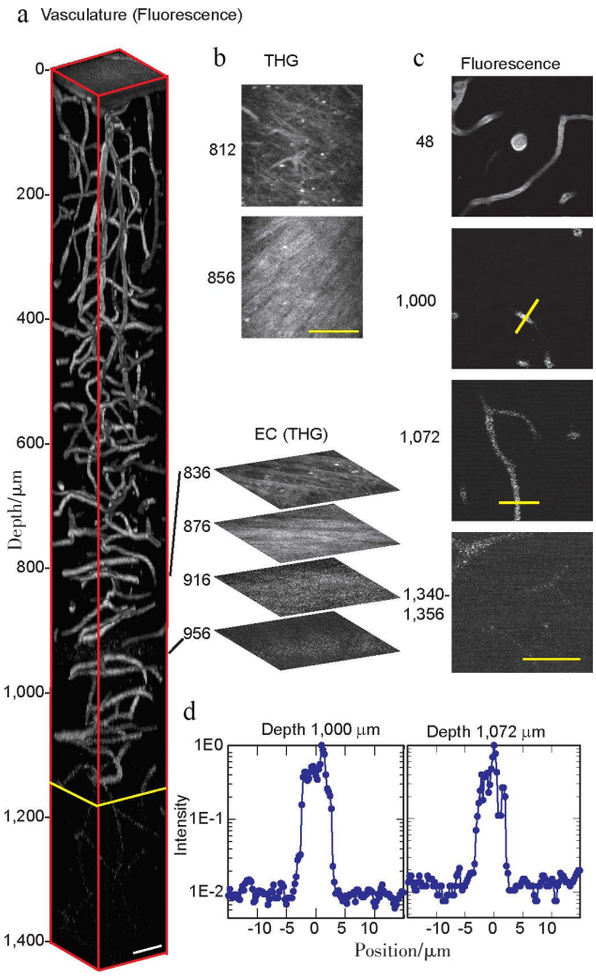

Fig.5a was the three-dimensional reconstruction of 3PM images of the brain in an FVB/N mouse. The external capsule (EC) extended from 840 to 956 mm below the surface of the brain. Frames deeper than 1 136 mm (yellow line) were normalized to the frame at 1 136 mm; all the other frames were individually normalized. The expanded optical sections to the right were the representative THG images from the external capsule region of the brain. Fig.5b and c were normalized x-y frames of the THG and fluorescence signal at various depths. The bottom frame in Fig.5c was a z-projection of 20 mm. The fluorescence profiles of the lines across the vessels in the middle two panels in Fig.5c were displayed in semi-logarithmic plots (Fig.5d), which were used for SBR calculation. The background was calculated by averaging the intensity values between 215 and 25 mm and between 5 and 15 mm.

图5 德克萨斯红葡萄糖标记的小鼠三维图像

Fig.5 *In vivo* 3PM images of brain vasculature in Texas-Red dextran labeled mouse (All scale bars: 50 mm)

共振成像的技术，可同时检测多个技术指标，能更准确地判断病症发展而且具备光学方法的高空间分辨率优势。成像结果表明，急性闭塞再灌注后，皮质区的散射特性发生变化；闭塞时，未灌注血管与皮质散射特性改变具有空间相关性，此区域最终可能发展为梗死区。未来这种成像平台有望用于脑血管疾病模型中，用来研究基因突变和基因治疗对这些模型的影响，同样也可以用于其它生物医学研究领域，如肿瘤研究等。

4.3 光声成像

光声成像结合了光学成像的高空间分辨率和声学成像穿透深的优点，成像的空间分辨率可达微米级[30]。具有光学分辨率的光声显微镜（OR-PAM）被应用于活体小鼠的脑功能成像。Hu等[31]采用近衍射限制的明场光学照明实现微米级横向分辨率，利用双波长测量提取血氧信息，成像结果可以清晰看到血液在进入动脉和静脉之后的血氧饱和度变化情况（图7）。该研究首次实现了完整头骨下精确到单根血管的功能性脑血管成像。

4.4 受激发射耗尽（Stimulated Emission Depletion, STED）

共聚焦显微镜或者多光子显微镜，仍然会受到光学衍射极限的限制，无法分辨被测样品200 nm以下的细节。STED与随机光学重建显微是目前在生物医学领域应用最为广泛的超分辨成像方法，然而受到成像速度、激发光强度等多种因素的限制，活体成像的研究还较少。Berning等[32]利用STED成像方法观察活体小鼠脑皮层的神经元以及神经元的细微动态变化，以488 nm激光作为激发光，592 nm环形激光作为耗尽光，形成的光斑通过正置显微镜成像系统对小鼠的神经元细胞（转染了Thy1-EYFP）进行成像（图8）。图8a是成像系统的结构示意图，图8b是对玻璃下方10~15 μm位置的体感皮质层的树突进行成像，图8c是每隔7~8 min成像获得的动态图像序列，该序列可以揭示成年小鼠树突棘形态随时间的形态变化情况。图片的分辨率远高于现有商用的共聚焦显微镜，与光学视窗技术相结合，STED将在活体脑成像中发挥更大的作用。

5 颅骨视窗在脑部研究中的典型应用

颅骨视窗优良的实时监测特性，使其广泛应用于长时间活体脑组织观察，包括正常神经细胞的生长、环路形成及可塑性研究，脑部疾病的发生发展机制研究，以及疾病治疗药物的疗效评价等，本文选取典型应用介绍如下。

5.1 对疾病发病机制及药物的研究

偏头痛是一种常见的多因素、神经血管发作病，病因不明。目前病理学上的主要解释为大脑皮层的兴奋度增强，以及脑干中三叉神经核里的神经元痛感控制异常[33]，颅外动脉的血管舒张也被认为是重

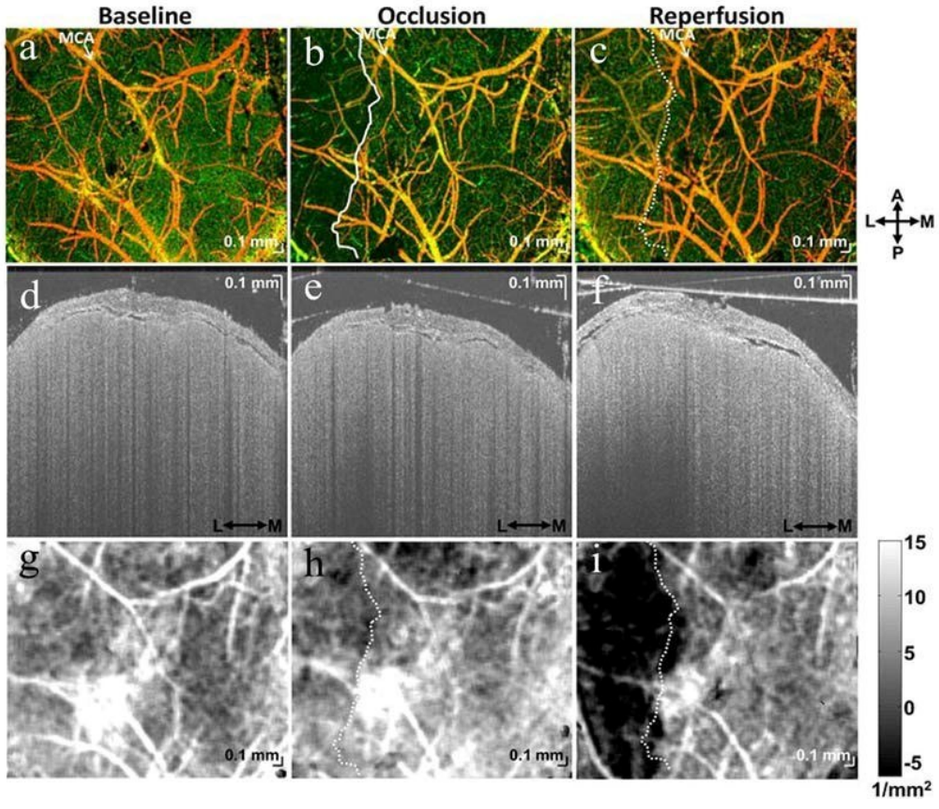

fMCAO: Filament middle cerebral artery occlusion; OCT: Optical coherence tomography; Fig.6a-c were OCT angiograms at baseline, during fMCAO, and 60 minutes after filament withdrawal, respectively. During fMCAO (Fig.6b), a capillary non-perfusion region was apparent, as demarcated with a solid white line. Fig.6d-f were OCT cross-sectional images on a logarithmic scale, with minor differences in alignment, showing the changing signal characteristics in the lateral portion of the cranial window after reperfusion (Fig.6f). Fig.6g-i were the images of the curvature of the OCT signal *vs*. depth at baseline. During fMCAO and 60 minutes after reperfusion showed this evolution. In Fig.6h-i, the capillary non-perfusion boundary from (Fig.6b) was shown as a dotted white line. In particular, the tissue with anomalous scattering properties (i.e., the log OCT signal *vs*. depth is concave down) after reperfusion corresponded well to the non-perfusion tissue during fMCAO. No comparable changes were observed in the contralateral hemisphere.

图6　fMCAO期间的毛细血管非灌注预测细胞散射信号变化最终导致梗死

Fig.6 Capillary non−perfusion during fMCAO predicts cellular scattering changes leads to eventual infarction.

要致病原因[34]。使用颅骨视窗技术可以清晰地观察到颅外动脉的血管扩张，既可以用于探究偏头痛的致病机理，也可以实时观察偏头痛药物的治疗效果及作用过程，大幅降低药物开发周期。Petersen等[4, 35]研究了降钙素基因相关肽在三叉神经血管系统中对偏头痛的发病机制的作用，研究表明该降钙素基因相关肽受体拮抗剂BIBN4096BS在治疗急性偏头痛中有较明显疗效，能有效地防止CGRP诱导的头痛和颅外血管舒张。使用颅骨视窗技术能实时观察拮抗剂对急性偏头痛的治疗过程，为研发新的治疗药物并进行药物评估提供新的思路。

5.2 对进行性疾病的实时观测

阿尔兹海默症病是一种进行性的神经功能障碍，大脑中的老年斑块和神经纤维缠结与其发病机理相关[36]。阿尔兹海默症的一个显著病理特征是淀粉样蛋白斑块的形成。淀粉样前体蛋白（Amyloid precursor Protein, APP）是一个穿过神经细胞膜的跨膜蛋白质，对于神经元的生长、存活和受伤后的修复非常重要[37]。β-淀粉样蛋白质是APP中较大的蛋白质片段，淀粉样蛋白斑块主要由β-淀粉样蛋白聚集而成。由于尚未探明的原因导致APP被酵素切成几个较小的片段纤维和β-淀粉样蛋白的增加，导致其在神经元外聚集形成淀粉蛋白斑块[38]。利用颅骨视窗技术可以清晰地观察蛋白质斑块的生长动力学，以及影响其生长的因素和周围组织对其的响应等[39-40]。有研究发现小胶质细胞会快速增殖聚集围绕在蛋白斑周围，清除淀粉样蛋白斑块，这为阿茨海默病的干预治疗提供了一个新的思路[41]。Yan等[42]

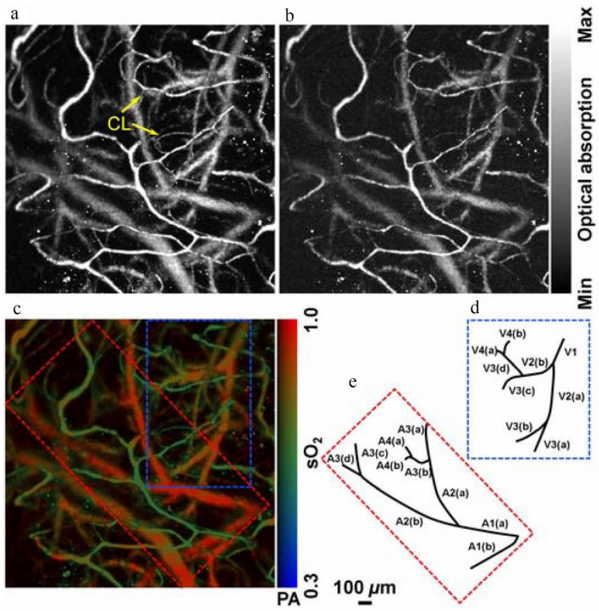

a: MAP image acquired at 570 nm; b: MAP image acquired at 578 nm; c: Vessel-by-vessel sO_2 mapping; d: A venular tree with branching orders boxed by blue dashed lines in Fig.7c; e: An arteriolar tree with branching orders boxed by red dashed lines in Fig.7c; The calculated sO_2 values were shown in the color bar photoacoustic signal amplitude.

图7 小鼠脑毛细血管的活体功能OR-PAM成像

Fig.7 *In vivo* functional optical-resolution photoacoustic microscopy imaging of mouse brain microvasculature through an intact skull

报道了间质中β-淀粉样蛋白浓度，以及反应性神经胶质增生对淀粉蛋白斑块生长的影响（图9）。得出斑块扩增速度与其本身大小正相关，减少β淀粉样蛋白浓度与反应性神经胶质增生均对斑块有抑制作用。

5.3 对突触生长、神经环路建立的观测以及神经功能研究

在大脑皮层中，神经回路的形成和退化与突触的可塑性有关。为了理解神经元细胞以及神经回路的工作机制，需要对神经元细胞或者神经回路的细微结构变化进行长时间反复成像。研究人员利用颅骨视窗，结合双光子激光扫描显微镜及基因编码荧光蛋白，实现了对大脑以及神经元结构的高分辨率成像（图10）[43-44]。Mank等[45]利用基因编码的钙指示器进一步观察神经细胞荧光情况变化，结合双光子扫描显微镜观察神经元功能的改变，这对于理解神经细胞可塑性、神经再生以及疾病的发生机制提供了崭新的思路。Andermann等[46]和Kuhlman等[47]则利用视窗研究了视觉神经区域的调节响应机制，并观察了视觉皮层的精细结构。Prakash等[48]和Packer等[49]报道了通过红移视蛋白的共表达和遗传编码的钙指示剂进行同时操纵和记录的多个神经元细胞活体高分辨率成像策略。

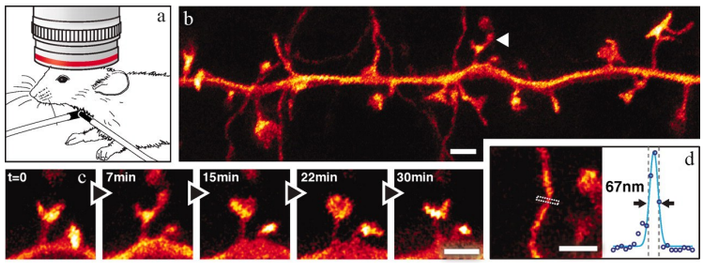

STED: Stimulated emission depletion; a: Anesthetized mouse under the objective lens (63×, NA 1.3, glycerol immersion) with tracheal tube; b-d: Projected volumes of dendritic and axonal structures revealed temporal dynamics of spine morphology with an approximately fourfold improved resolution compared with diffraction-limited imaging; Curve was a three-pixel-wide line profile fitted to raw data with a Gaussian.

图8 STED显微镜对小鼠体感皮层EYFP标记的神经元成像

Fig.8 STED microscopy in themolecular layer of the somatosensory cortex of a mouse with EYFP-labeled neurons (Scale bars: 1 mm)

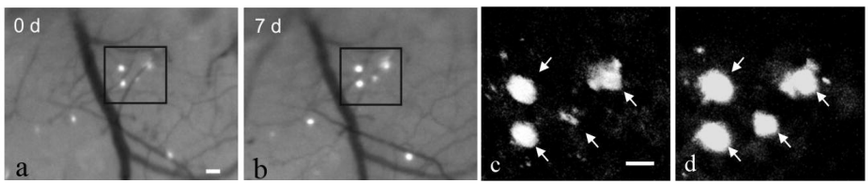

a-b: Epifluorescence micrographs of 4 plaques labeled with methoxy-X04 and imaged over a 7 d interval in the brain of a 6-month-old APP/PS1 mouse; c-d: Multiphoton micrographs of those same 4 plaques illustrated the growth of individual plaques over time.

图9 多光子显微镜观察活体淀粉样蛋白斑块的生长

Fig.9 Growth of individual amyloid plaques observed with serial *in vivo* multiphoton microscopy (Scale bars: 20μm)

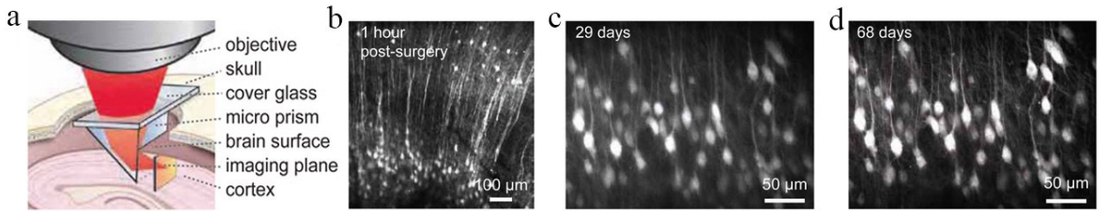

Fig.10a was the illustration of beam path through a prism implanted into neocortex. The reflective hypotenuse of the prism converted the horizontal imaging plane into a vertical plane. Fig.10b-d were the anatomical images of cortex taken though a prism at different times after surgery in a Thy1-YFP mouse. Within the first hour after prism insertion, cell bodies in layers 2/3 and 5, and neuronal processes throughout the cortical depth, were visible in a single frame taken 200 microns lateral from the prism face (left panel). An increase in imaging quality over time was evident on the same population of layer 5 neurons at 29 and 68 days after surgery (middle and right panel, respectively. Images were maximum projections over 76 frames taken from 40 mm to 270 mm lateral to the prism face.).

图10　微型棱镜对表层及深层神经元成像

Fig.10 Superficial and deep cortical layers imaged in a single plane using a microprism

5.4 脑部疾病疗效评价

细胞粘附分子是细胞维持形态与功能，参与细胞与细胞间或细胞与细胞外基质作用的分子。多种癌组织中细胞粘附分子减少会造成癌细胞脱落，癌细胞得以侵袭和转移。动脉瘤性蛛网膜下腔出血造成白细胞的运输增强。Xu等[50]以一种选择性VAP-1阻断剂LJP-1586[Z-3-fluoro-2-(4-methoxybenzyl), Z-3-氟-2-(4甲氧苄基)烯丙基胺盐酸盐]利用FITC葡聚糖观察动脉瘤性蛛网膜下腔出血下白细胞粘附性的变化，发现血管粘附蛋白-1(Vascular Adhesion Protein-1, VAP-1)增强了白细胞的粘附性。Yuan等[51]和Gaber等[52]则使用FITC葡聚糖评估了辐射对血脑屏障的影响，分别用5种不同大小的FITC葡聚糖分子(4.4~150.0 kDa)来研究血脑屏障渗透性的改变，发现只有150 kDa大小的分子不能透过血脑屏障，而在辐射2 h后发现白细胞粘附性上升，至24 h达到最大(图11)。Frank和Hong等利用药物与辐射对肿瘤进行协同治疗或消除炎症，比单一药物具有更显著的疗效。Asuthkar等[53-54]则报道了电离辐射下基质金属蛋白酶9(Matrix Metalloproteinase-9, MMP-9)与多配体聚糖-1(Syndecan-1, SDC1)、MicroRNA-494之间的调节环路影响诱导髓母细胞瘤细胞凋亡的能力以及MMP-9对于MicroRNA-211的影响以及对胶质母细胞瘤的治疗效果。

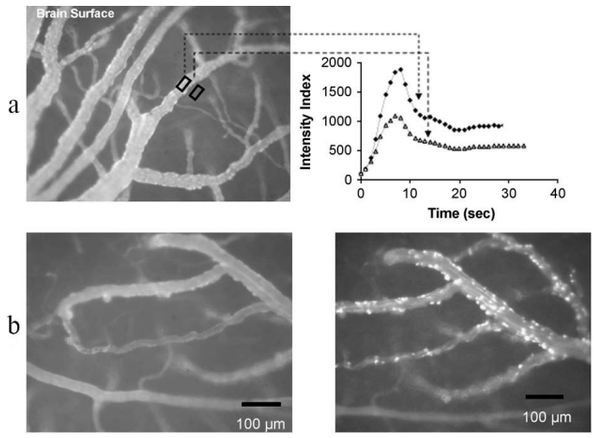

Fig.11a was the fluorescent image of pial vasculature after injection with FITC-dextran (4.4-150.0 kDa) (left panel). The intensity of fluorescence from the vessel (solid diamonds) and nearby tissue (open triangles) was recorded from a typical region of interest (right panel). In fig.11b, leukocyte adhesion was determined before (left panel) and 24 h after (right panel) exposure to 20 Gy irradiation.

图11 渗透性与白细胞特性

Fig.11 Permeability and leukocyte properties

6 总结与展望

小鼠颅骨视窗为微米尺度下原位观察神经元细胞形态及功能提供了新的技术方法，结合荧光探针和光学显微成像方法，研究人员能够直接在活体水平上获得大脑表面和深层组织与细胞的局部动态信息，开展疾病发生机制、药物作用机制以及细胞结构和功能等方面的研究，显著节约了研究时间和成本。颅骨视窗技术所具有的独特优势，推动了科研人员对神经元及脑部疾病(如偏头痛、阿尔兹海默症等)发生发展机制的了解，已成为神经生物学的重要研究手段。然而，目前常用的颅骨视窗也有其应用局限，对颅骨进行打磨的颅钻多是手持式，且小鼠颅骨较薄，打磨过程中较难把握控制具体打磨程度，易发生轻微炎症反应，若能构建包括显微镜和颅钻的自动化平台，则可显著提高实验成功率，此外，结合颅骨组织透明技术、传感器阵列技术等[55-56]，则可能在减少对小鼠损伤的同时获得脑内更高分辨率、更

多维度的信息，为人类理解大脑的工作机理提供更加实用有效的帮助。

【参考文献】

[1] ROSENBLUM W I, ZWEIFACH B W. Cerebral microcirculation in the mouse brain. Spontaneous and drug-induced changes in flow and vascular diameter[J]. Arch Neurol-chicago, 1963, 9: 414.

[2] GRUTZENDLER J, KASTHURI N, GAN W B. Long-term dendritic spine stability in the adult cortex[J]. Nature, 2002, 420(6917): 812.

[3] SHIH A Y, MATEO C, DREW P J, et al. A polished and reinforced thinned-skull window for long-term imaging of the mouse brain[J]. J Vis Exp, 2012(61): 3742.

[4] PETERSEN K A, BIRK S, DOODS H, et al. Inhibitory effect of bibn4096bs on cephalic vasodilatation induced by CGRP or transcranial electrical stimulation in the rat[J]. Br J Pharmacol, 2004, 143(6): 697-704.

[5] HORTON N G, KE W, KOBAT D, et al. *In vivo* three-photon microscopy of subcortical structures within an intact mouse brain[J]. Nat Photonics, 2013, 7(3): 205-209.

[6] MIYAWAKI A. Innovations in the imaging of brain functions using fluorescent proteins[J]. Neuron, 2005, 48(2): 189-199.

[7] FORBES H S. The cerebral circulation. I. Observation and measurement of pial vessels[J]. Febs Lett, 1928, 388(1): 73-75.

[8] KUSCHINSKY W, WAHL M. Comparison between the open skull and the cranial window preparation for studying the cerebral microcirculation[J]. Microvasc Res, 1980, 19(19): 385-386.

[9] DREW P J, SHIH A Y, DRISCOLL J D, et al. Chronic optical access through a polished and reinforced thinned skull[J]. Nat Methods, 2010, 7(12): 981.

[10] GOLDEY G J, ROUMIS D K, GLICKFELD L L, et al. Removable cranial windows for long-term imaging in awake mice[J]. Nat Protoc, 2014, 9(11): 2515-2538.

[11] MARKER D F, TREMBLAY M E, LU S M, et al. A thin-skull window technique for chronic two-photon *in vivo* imaging of murine microglia in models of neuroinflammation[J]. J Vis Exp, 2010, 43(43): 2059.

[12] LEVASSEUR J E, WEI E P, RAPER A J, et al. Detailed description of a cranial window technique for acute and chronic experiments[J]. Stroke, 1975, 6(3): 308.

[13] MORII S, NGAI A C, WINN H R. Reactivity of rat pial arterioles and venules to adenosine and carbon dioxide: with detailed description of the closed cranial window technique in rats[J]. J Cereb Blood Flow Metab, 1986, 6(1): 34-41.

[14] SHIH A Y, MATEO C, DREW P J, et al. A polished and reinforced thinned-skull window for long-term imaging of the mouse brain[J]. J Vis Exp, 2012(61): e3742.

[15] KELLY E A, MAJEWSKA A K. Chronic imaging of mouse visual cortex using a thinned-skull preparation[J]. J Vis Exp, 2010(44): 2060.

[16] DOMBECK D A, KHABBAZ A N, COLLMAN F, et al. Imaging large-scale neural activity with cellular resolution in awake, mobile mice[J]. Neuron, 2007, 56(1): 43.

[17] ROVAINEN C M, WOOLSEY T A, BLOCHER N C, et al. Blood flow in single surface arterioles and venules on the mouse somatosensory cortex measured with videomicroscopy, fluorescent dextrans, nonoccluding fluorescent beads, and computer-assisted image analysis [J]. J Cereb Blood Flow Metab, 1993, 13(3): 359.

[18] CHALFIE M, TU Y, EUSKIRCHEN G, et al. Green fluorescent protein as a marker for gene expression[J]. Science, 1994, 263(5148): 802-805.

[19] ORM M, CUBITT A B, KALLIO K, et al. Crystal structure of the aequorea victoria green fluorescent protein[J]. Science, 1996, 273 (5280): 1392-1395.

[20] GIEPMANS B N, ADAMS S R, ELLISMAN M H, et al. The fluorescent toolbox for assessing protein location and function[J]. Science, 2006, 312(5771): 217-224.

[21] FENG G, MELLOR R H, BERNSTEIN M, et al. Imaging neuronal subsets in transgenic mice expressing multiple spectral variants of GFP [J]. Neuron, 2000, 28(1): 41-51.

[22] KIENAST Y, VON B L, FUHRMANN M, et al. Real-time imaging reveals the single steps of brain metastasis formation[J]. Nat Med, 2010, 16(1): 116.

[23] CHEN T, WARDILL T J, SUN Y, et al. Ultrasensitive fluorescent proteins for imaging neuronal activity[J]. Nature, 2013, 499(7458): 295-300.

[24] GUO L, XIONG H, KIM J I, et al. Dynamic re-wiring of neural circuits in the motor cortex in mouse models of Parkinson's disease[J]. Nat Neurosci, 2015, 18(9): 1299-1309.

[25] CHENG M Y, WANG E H, WOODSON W J, et al. Optogenetic neuronal stimulation promotes functional recovery after stroke[J]. Proc Natl Acad Sci USA, 2014, 111(35): 12913-12918.

[26] HELMCHEN F, DENK W. Deep tissue two-photon microscopy[J]. Nat Methods, 2005, 2(2): 932-940.

[27] XU H, PAN F G, GAN W. Choice of cranial window type for *in vivo* imaging affects dendritic spine turnover in the cortex [J]. Nat Neurosci, 2007, 10(5): 549.

[28] XU T, YU X, PERLIK A J, et al. Rapid formation and selective stabilization of synapses for enduring motor memories[J]. Nature, 2009, 462(7275): 915-919.

[29] SRINIVASAN V J, MANDEVILLE E T, CAN A, et al. Multiparametric, longitudinal optical coherence tomography imaging reveals acute injury and chronic recovery in experimental ischemic stroke[J]. PLoS One, 2013, 8(8): e71478.

[30] WANG L V, HU S. Photoacoustic tomography: *in vivo* imaging from organelles to organs[J]. Science, 2012, 335(6075): 1458.

[31] HU S, MASLOV K, TSYTSAREV V, et al. Functional transcranial brain imaging by optical-resolution photoacoustic microscopy[J]. J Biomed Opt, 2011, 14(4): 040503.

[32] BERNING S, WILLIG K I, STEFFENS H, et al. Nanoscopy in a living mouse brain[J]. Science, 2012, 335(6068): 551.

[33] DODICK D W, GARGUS J J. Why migraines strike[J]. Sci Am, 2008, 299(2): 56-63.

[34] SHEVEL E. The extracranial vascular theory of migraine-a great story confirmed by the facts[J]. Headache, 2011, 51(3): 409-417.

[35] PETERSEN K A, LASSEN L H, BIRK S, et al. Bibn4096bs antagonizes human alpha-calcitonin gene related peptide-induced headache and extracerebral artery dilatation[J]. Clin Pharmacol Ther, 2005, 77(3): 202-213.

[36] TIRABOSCHI P, HANSEN L A, THAL L J, et al. The importance of neuritic plaques and tangles to the development and evolution of AD [J]. Neurology, 2004, 62(11): 1984.

[37] PRILLER C, BAUER T, MITTEREGGER G, et al. Synapse formation and function is modulated by the amyloid precursor protein[J]. J Neurosci, 2006, 26(27): 7212.

[38] OHNISHI S, TAKANO K. Amyloid fibrils from the viewpoint of protein folding[J]. Cell Mol Life Sci, 2004, 61(5): 511-524.

[39] SAVONENKO A, XU G M, MELNIKOVA T, et al. Episodic-like memory deficits in the APPswe/PS1dE9 mouse model of Alzheimer's disease: relationships to beta-amyloid deposition and neurotransmitter abnormalities[J]. Neurobiol Dis, 2005, 18(3): 602-617.

[40] STERN E A, BACSKAI B J, HICKEY G A, et al. Cortical synaptic

integration *in vivo* is disrupted by amyloid- beta plaques［J］. J Neurosci, 2004, 24(19): 4535.

［41］BOLMONT T, HAISS F, EICKE D, et al. Dynamics of the microglial/amyloid interaction indicate a role in plaque maintenance［J］. J Neurosci, 2008, 28(16): 4283.

［42］YAN P, BERO A W, CIRRITO J R, et al. Characterizing the appearance and growth of amyloid plaques in app/ps1 mice［J］. J Neurosci, 2009, 29(34): 10706.

［43］ANDERMANN M L, GILFOY N B, GOLDEY G J, et al. Chronic cellular imaging of entire cortical columns in awake mice using microprisms［J］. Neuron, 2013, 80(4): 900-913.

［44］HOLTMAAT A J, TRACHTENBERG J T, WILBRECHT L, et al. Transient and persistent dendritic spines in the neocortex *in vivo*［J］. Neuron, 2005, 45(2): 279.

［45］MANK M, SANTOS A F, DIRENBERGER S, et al. A genetically encoded calcium indicator for chronic *in vivo* two-photon imaging［J］. Nat Methods, 2008, 5(9): 805.

［46］ANDERMANN M L, KERLIN A M, ROUMIS D K, et al. Functional specialization of mouse higher visual cortical areas［J］. Neuron, 2011, 72(6): 1025.

［47］KUHLMAN S J, OLIVAS N D, TRING E, et al. A disinhibitory microcircuit initiates critical-period plasticity in the visual cortex［J］. Nature, 2013, 501(7468): 543-546.

［48］PRAKASH R, YIZHAR O, GREWE B, et al. Two-photon optogenetic toolbox for fast inhibition, excitation and bistable modulation［J］. Nat Methods, 2012, 9(12): 1171-1179.

［49］PACKER A M, RUSSELL L E, DALGLEISH H W, et al. Simultaneous all-optical manipulation and recording of neural circuit activity with cellular resolution *in vivo*［J］. Nat Methods, 2015, 12(2): 140.

［50］XU H L, GARCIA M, TESTAI F, et al. Pharmacologic blockade of vascular adhesion protein-1 lessens neurologic dysfunction in rats subjected to subarachnoid hemorrhage［J］. Brain Res, 2014, 1586: 83.

［51］YUAN H, GABER M W, MCCOLGAN T, et al. Radiation-induced permeability and leukocyte adhesion in the rat blood-brain barrier: modulation with anti-icam-1 antibodies［J］. Brain Res, 2003, 969(1-2): 59.

［52］GABER M W, YUAN H, KILLMAR J T, et al. An intravital microscopy study of radiation-induced changes in permeability and leukocyte- endothelial cell interactions in the microvessels of the rat pia mater and cremaster muscle［J］. Brain Res Protoc, 2004, 13 (1): 1-10.

［53］ASUTHKAR S, VELPULA K K, CHETTY C, et al. Epigenetic regulation of miRNA-211 by MMP-9 governs glioma cell apoptosis, chemosensitivity and radiosensitivity［J］. Oncotarget, 2012, 3(11): 1439.

［54］ASUTHKAR S, VELPULA K K, NALLA A K, et al. Irradiation-induced angiogenesis is associated with an MMP- 9- miR- 494-syndecan-1 regulatory loop in medulloblastoma cells［J］. Oncogene, 2014, 33(15): 1922-1933.

［55］FUJITA H, MATSUURA T, YAMADA K, et al. A sealed cranial window system for simultaneous recording of blood flow, and electrical and optical signals in the rat barrel cortex［J］. J Neurosci Meth, 2000, 99(1-2): 71-78.

［56］HONG G, DIAO S, CHANG J, et al. Through-skull fluorescence imaging of the brain in a new near-infrared window［J］. Nat Photonics, 2014, 8(9): 723.

（编辑：谭斯允）